32nd URSI GASS, Montreal, 19-26 August 2017

Shared-Aperture Modulated Metasurface Antennas

David González Ovejero(1), Gabriele Minatti(2), Marco Faenzi(2), Francesco Caminita(2),(3), Enrica Martini(2),(3), and Stefano Maci*(2)
(1) Institut d'Électronique et de Télécommunications de Rennes - UMR CNRS 6164, 35042 Rennes, France
(2) Department of Information Engineering and Mathematics, University of Siena, 53100 Siena, Italy
(3) Wave Up S.r.l., Florence 50126, Italy

Abstract

This paper describes the design multibeam or dual-band antennas using just a single metasurface (MTS) aperture. An example of multi-beam antenna is presented, it is based on a superposition of modulation patterns, and presents a multi-source feeding scheme. The elements of the objective surface impedance tensor are derived in closed-form, and numerical results based on the Method of Moments are presented for validation.

1. Introduction

In recent years, metasurface (MTS) [1],[2] theory and applications have undergone an unprecedented development. MTSs have been applied to design structures at microwave frequencies [1], in the Terahertz range [2, Sec. VII] or at optical wavelengths [3]. Regarding the applications at hand, they can be roughly classified in three groups: 1) the manipulation of surface wave (SW) wavefronts [4], 2) the control of field transmission [5], and 3) the design of aperture antennas [6]-[7]. In this paper, we will focus in the latter application.

Modulated MTS antennas present several characteristics that make them very attractive, among which it is worth noting their capability of providing high gains with low profile and low weight structures [7]. In this class of antennas, a SW is gradually radiated by periodically modulating an (equivalent) surface impedance tensor on the aperture plane. The periodic modulation is chosen so that the (-1) indexed Floquet mode enters in the visible region. At sub-millimeter waves, the modulation can be achieved by using textured metallic structures [8]. Nonetheless, the use of printed patches on a grounded dielectric slab is preferred in the microwave range [6]-[7]. We will analyze the case of circular apertures of radius a, in which the modulation of the surface impedance is achieved by changing the shape and orientation of sub-wavelength patches printed on a grounded slab with relative permittivity ε_r and thickness h (see Fig. 1). In the following, we will represent the cladding as a sheet transition IBC [2],[9] given by the tensor $\underline{\underline{\mathbf{X}}}$, which relates the average of the E-field $\mathbf{E}_t$ on either side of the MTS with the difference in the tangential components of the H-field on both sides of the sheet as:

$$\mathbf{E}_t = j\underline{\underline{\mathbf{X}}}\cdot\hat{\mathbf{z}}\times\left(\mathbf{H}_t\big|_{z=0^+} - \mathbf{H}_t\big|_{z=0^-}\right) = j\underline{\underline{\mathbf{X}}}\cdot\mathbf{J} \quad , \qquad (1)$$

The difference between the tangential H-fields can be interpreted as the current flowing in the cladding. In the next section, we will provide closed-form expressions for $\underline{\underline{\mathbf{X}}}$ which lend the MTS the desired functionality.

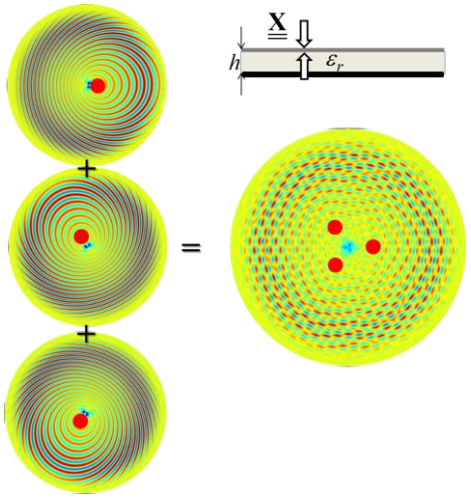

Figure 1 Component $X_{\rho\rho}$ of the surface reactance tensor of a MTS aperture which provides three beams by three sources and aperture sharing by a superposition of modulated impedance patterns. The inset shows the reference structure composed of a grounded dielectric slab, printed with sub-wavelength metal patches.

2. Shared aperture MTS antennas

The simplest way of achieving several functionalities with the same aperture consists in dividing the aperture in angular sectors, each sector being associated with a different feature, as done in [10],[11] by using isotropic MTSs, and in [12, Sec. II] by applying anisotropic MTSs and control of the amplitude to increase aperture efficiency [13].

Conversely, we will study here the cases in which the whole aperture is shared by a superposition of individual modulations (see Fig. 1), which correspond to those required to obtain the desired beams. In this class of shared-aperture MTS, the (-1) term of the Floquet-wave expan-

sion, which provides the tangential electric field in the aperture plane, can be written as:

$$\mathbf{E}^{(-1)}(\boldsymbol{\rho}) = \sum_{n=1}^{N} \mathbf{e}_n \; E_0 e^{-\mathrm{j}k\,\hat{\mathbf{r}}_n\cdot\boldsymbol{\rho}} e(\rho) u(a-\rho) \qquad (2)$$

where $\boldsymbol{\rho}$ is the observation point given by (ρ,ϕ) in cylindrical coordinates, N is the number of beams, and $u(x)$ is the unit step function. The unit vector

$$\hat{\mathbf{r}}_n = \sin\theta_n\cos\varphi_n\hat{\mathbf{x}} + \sin\theta_n\sin\varphi_n\hat{\mathbf{y}} + \cos\theta_n\hat{\mathbf{z}} \qquad (3)$$

determines the direction of the n-th beam, and $\mathbf{e}_n$ gives its polarization. For instance, one has for circularly polarized beam in the direction (θ_n,φ_n)

$$\begin{aligned}\mathbf{e}_n = {} & \hat{\mathbf{x}}\left(\cos\theta_n\cos\varphi_n \mp \mathrm{j}\sin\varphi_n\right) \\ & + \hat{\mathbf{y}}\left(\cos\theta_n\sin\varphi_n \pm \mathrm{j}\cos\varphi_n\right)\end{aligned} \qquad (4)$$

The upper signs in (4) correspond to right-handed circular polarization (RHCP), whereas the lower ones stand for left-handed circular polarization (LHCP).

In the first instance, we will consider a SW source at $\boldsymbol{\rho}_n$, which will generate the n-th beam in (2) when it is excited. The observation point in the aperture is given by $\mathbf{R}_n = \boldsymbol{\rho} - \boldsymbol{\rho}_n$ in relative coordinates, and the unit vectors centered at the n-th source are

$$\hat{\boldsymbol{\kappa}}_n = (\boldsymbol{\rho} - \boldsymbol{\rho}_n)/R_n, \;\; \hat{\boldsymbol{\gamma}}_n = (\hat{\mathbf{z}}\times\hat{\boldsymbol{\kappa}}_n) \qquad (5)$$

where $R_n = |\boldsymbol{\rho} - \boldsymbol{\rho}_n|$. Then, the local values of the tensor elements needed to generate the n-th beam with circularly polarization can be written as

$$\begin{aligned}
X_{\kappa\kappa}^{(n)}(\mathbf{R}_n) &= X_0\left[1 + m_\kappa^{(n)}(\mathbf{R}_n)\sin\left(\beta_{sw}\kappa_n - k\,\hat{\mathbf{r}}_n\cdot\boldsymbol{\kappa}_n \pm \Phi_\kappa^{(n)}\right)\right] \\
X_{\kappa\gamma}^{(n)}(\mathbf{R}_n) &= X_0\, m_\gamma^{(n)}(\mathbf{R}_n)\sin\left(\beta_{sw}\kappa_n - k\,\hat{\mathbf{r}}_n\cdot\boldsymbol{\kappa}_n \pm \Phi_\gamma^{(n)}\right) \\
X_{\gamma\gamma}(\mathbf{R}_n) &= \frac{X_0}{|\hat{\mathbf{e}}_n\cdot\hat{\boldsymbol{\kappa}}_n|^2}\left[1 - m_\kappa^{(n)}(\mathbf{R}_n)\sin\left(\beta_{sw}\kappa_n - k\,\hat{\mathbf{r}}_n\cdot\boldsymbol{\kappa}_n \pm \Phi_\kappa^{(n)}\right)\right] \\
m_\chi^{(n)}(\mathbf{R}_n) &= m(\mathbf{R}_n)|\hat{\mathbf{e}}_n\cdot\hat{\boldsymbol{\chi}}_n| \\
\Phi_\kappa^{(n)} &= \tan^{-1}\left[\mathrm{Im}(\hat{\mathbf{e}}_n\cdot\hat{\boldsymbol{\chi}}_n)/\mathrm{Re}(\hat{\mathbf{e}}_n\cdot\hat{\boldsymbol{\chi}}_n)\right] \;\; \chi = \kappa,\gamma
\end{aligned} \qquad (6)$$

where $m(\mathbf{R}_n)$ is the function used for amplitude control, the unit vectors $\hat{\mathbf{e}}_n$ have been defined in (4), and the upper/lower sign stand for a RHCP/LHCP polarization in the corresponding beam.

It has been proved in [12] that by combining the modulations in (6) for each beam as

$$\begin{aligned}\underline{\underline{\mathbf{X}}} = \frac{1}{N}\sum_{n=1}^{N}\Big(& \hat{\boldsymbol{\kappa}}_n\hat{\boldsymbol{\kappa}}_n X_{\kappa\kappa}^{(n)} + \left(\hat{\boldsymbol{\kappa}}_n\hat{\boldsymbol{\gamma}}_n + \hat{\boldsymbol{\gamma}}_n\hat{\boldsymbol{\kappa}}_n\right) X_{\kappa\gamma}^{(n)} \\ & + \hat{\boldsymbol{\varphi}}_n\hat{\boldsymbol{\varphi}}_n X_{\gamma\gamma}^{(n)}\Big) u(a-\rho)\end{aligned} \qquad (7)$$

one can attain the objective tangential electric field in (2). Although (7) addresses a general case with N beams, it should be noted that the superposition of modulation patterns leads to a degradation of the performance of the synthesized beams for an increasing number of beams, typically $N \le 4$. An analogous approach can be used to obtain dual-band MTSs by superimposing the impedance modulations relevant to each frequency. This case will be further discussed at the conference.

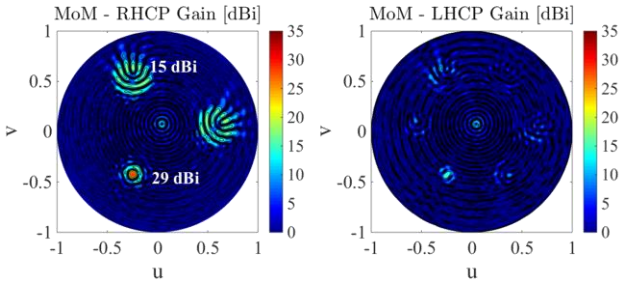

Figure 2 (a) RHCP and (b) LHCPs gain in the u-v plane for the reactance tensor given by (7) with N=3, (θ_1=30°, φ_1=0), (θ_2=30°, φ_2=120°), and (θ_3=30°, φ_3=240°) and sources in $\boldsymbol{\rho}_1 = 1.7\lambda\hat{\mathbf{x}}$, $\boldsymbol{\rho}_2 = -0.4\lambda\hat{\mathbf{x}} + 0.7\lambda\hat{\mathbf{y}}$, and $\boldsymbol{\rho}_3 = -0.4\lambda\hat{\mathbf{x}} - 0.7\lambda\hat{\mathbf{y}}$, respectively.

3. Numerical Examples

In this section, an example is presented of multibeam MTS antenna, which uses three feeding points to synthesize three independent RHCP beams. The radius of the aperture is a=12λ, and the substrate has ε_r=9.8 and thickness h=0.508mm. The location of the three phase centers are given by $\boldsymbol{\rho}_1 = 1.7\lambda\hat{\mathbf{x}}$, $\boldsymbol{\rho}_2 = -0.4\lambda\hat{\mathbf{x}} + 0.7\lambda\hat{\mathbf{y}}$, and $\boldsymbol{\rho}_3 = -0.4\lambda\hat{\mathbf{x}} - 0.7\lambda\hat{\mathbf{y}}$. In turn, the desired beam directions are (θ_1=30°, φ_1=0), (θ_2=30°, φ_2=120°), and (θ_3=30°, φ_3=240°). We have simulated the continuous sheet transition IBC obtained upon substitution of the aforementioned values in (7). We will only show results that correspond to the simulation of $\underline{\underline{\mathbf{X}}}$ with the method of moments (MoM) tool described in [14], owing to the excellent agreement shown in [12],[14] with the simulations of actual structures.

Fig. 2(a) and (b) show the u-v plane RHCP and LHCP far-fields, obtained by exciting a single VED located at $\boldsymbol{\rho}_3 = -0.4\lambda\hat{\mathbf{x}} - 0.7\lambda\hat{\mathbf{y}}$. One can see that the directivity peaks in direction of $\hat{\mathbf{r}}_3$ (θ_3=30°, φ_3=240°). The u-v plane radiation patterns for each one of the other 3 possible excitations are quite similar to the one in Fig. 2(a) and (b), except for a rotation, and are not reported here. In all the three cases, the active beam presents a gain of 29 dBi.

4. Conclusions

We have discussed different design possibilities offered by shared-aperture modulated metasurface antennas. Special emphasis has been put in designs which involve multiple sources. By exciting each source one will activate one beam at a time. The produced beams are quasi-orthogonal, which offers a significant advantage for processing signals impinging from different directions. The proposed approach can be used to design dual-band or

multi-beam high-gain antennas. The latter can be applied to Doppler radio-guides and radio altimeter systems.

5. Acknowledgements

The work of D. Gonzalez-Ovejero was supported by a Marie Curie International Outgoing Fellowship within the 7th European Community Framework Programme. The work of G. Minatti, M. Faenzi, F. Caminita, E. Martini and S. Maci has been supported by the European Space Agency (ESA-ESTEC, Noordwijk, The Netherlands) under contract 4000111496/14/NL/GLC/al "Low Complexity Data Downlink Antenna" and by the Army Research Laboratory under contract No. W911NF-15-1-0528.

6. References

1. S. Maci, G. Minatti, M. Casaletti, and M. Bosiljevac, "Metasurfing: Addressing Waves on Impenetrable metasurfaces," *IEEE Antennas Wireless Propag. Lett.*, **10**, 2011, pp. 1499–1502, doi: 10.1109/LAWP.2012.2183631.

2. C. Holloway, E. F. Kuester, J. Gordon, J. O'Hara, J. Booth, and D. Smith, "An Overview of the Theory and Applications of Metasurfaces: the two-dimensional Equivalents of Metamaterials," *IEEE Antennas Propag. Mag.*, **54**, 2, April 2012, pp. 10–35, doi: 10.1109/MAP.2012.6230714.

3. N. Yu et al., "Flat Optics: Controlling Wavefronts with Optical Antenna Metasurfaces," *IEEE J. Sel. Topics Quantum Electron.*, **19**, 3, May 2013, pp. 4700423, doi: 10.1109/JSTQE.2013.2241399.

4. M. Mencagli, E. Martini, D. González-Ovejero, and S. Maci, "Metasurfing by Transformation Electromagnetics," *IEEE Antennas Wireless Propag. Lett.*, **13**, October 2014, pp. 1767–1770, doi: 10.1109/LAWP.2014.2364981.

5. C. Pfeiffer and A. Grbic, "Metamaterial Huygens' Surfaces: Tailoring Wave Fronts with Reflectionless Sheets," Phys. Rev. Lett., **110**, May 2013, p. 197401, doi: 10.1103/PhysRevLett.110.197401.

6. B. H. Fong, J. S. Colburn, J. J. Ottusch, J. L Visher, and D. F. Sievenpiper, "Scalar and Tensor Holographic Artificial Impedance Surfaces," *IEEE Trans. Antennas Propag.*, **58**, 10, Oct. 2010, pp. 3212–3221, doi: 10.1109/TAP.2010.2055812.

7. G. Minatti et al., "Modulated Metasurface Antennas for Space: Synthesis, analysis and realizations," *IEEE Trans. Antennas Propag.*, **63**, 4, Apr. 2015, pp. 1288–1300, doi: 10.1109/TAP.2014.2377718.

8. D. González-Ovejero, T. J. Reck, C. D. Jung-Kubiak, M. Alonso-DelPino, and G. Chattopadhyay, "A Class of Silicon Micromachined Metasurface for the Design of High-Gain Terahertz Antennas," *Proc. IEEE AP-S Soc. Int. Symp.*, July 2016, doi: 10.1109/APS.2016.7696303.

9. E. F. Kuester, M. Mohamed, M. Piket-May, and C. Holloway, "Averaged Transition Conditions for Electromagnetic Fields at a Metafilm," *IEEE Trans. Antennas Propag.*, **51**, 10, Oct. 2003, pp. 2641–2651, doi: 10.1109/TAP.2003.817560.

10. Y. B. Li, X. Wan, B. G. Cai, Q. Cheng, T. J. Cui, "Frequency-Controls of Electromagnetic Multi-beam Scanning by Metasurfaces", *Scientific Reports*, **4**: 6921, 5, November 2014, doi:10.1038/srep06921.

11. D. González-Ovejero, G. Chattopadhyay, and S. Maci, "Multiple Beam Shared Aperture Modulated Metasurface Antennas" *Proc. IEEE AP-S Soc. Int. Symp.*, July 2016, doi: 10.1109/APS.2016.7695759.

12. D. González-Ovejero, G. Minatti, G. Chattopadhyay and S. Maci, "Multibeam by Metasurface Antennas," *IEEE Trans. Antennas Propag.*, in press.

13. G. Minatti, F. Caminita, E. Martini, M. Sabbadini, and S. Maci, "Synthesis of Modulated-Metasurface Antennas with Amplitude, Phase and Polarization Control," *IEEE Trans. Antennas Propag.*, **64**, 9, Sept. 2016, pp. 3907–3919, doi: 10.1109/TAP.2016.2589969.

14. D. González-Ovejero and S. Maci, "Gaussian Ring Basis Functions for the Analysis of Modulated Metasurface Antennas," *IEEE Trans. Antennas Propag.*, **63**, 9, Sept. 2015, pp. 3982–3993, doi: 10.1109/TAP.2015.2442585.